Clinical Chemistry 52:2
182–191 (2006)

Three Mutations (p.Q36H, p.G418fsX482, and g.IVS19-2A>C) in the Dual Oxidase 2 Gene Responsible for Congenital Goiter and Iodide Organification Defect

Viviana Varela,[1] Carina M. Rivolta,[1] Sebastián A. Esperante,[1]
Laura Gruñeiro-Papendieck,[2] Ana Chiesa,[2] and Héctor M. Targovnik[1*]

Background: **Iodide organification defects are associated with mutations in the dual oxidase 2 (*DUOX2*) gene and are characterized by a positive perchlorate discharge test. These mutations produce a congenital goitrous hypothyroidism, usually transmitted in an autosomal recessive mode.**

Methods: **We studied the complete coding sequence of the human *DUOX2* gene by single-strand conformational polymorphism (SSCP) analysis of DNA from 17 unrelated patients with iodide organification defects. Samples showing an aberrant pattern were directly sequenced. All mutations were validated by SSCP analysis. Finally, the effect of a splicing mutation was studied by construction of minigenes.**

Results: **Genomic DNA sequencing revealed 3 novel mutations [c.108G>C (p.Q36H), c.1253delG (p.G418fsX482), and g.IVS19-2A>C] and 1 previously reported mutation [c.2895-2898delGTTC (p.S965fsX994)] in 2 families with 1 (family 1) and 2 (family 2) affected members. This implies the inheritance of 2 compound heterozygous mutations, p.Q36H and p.S965fsX994 in family 1 and p.G418fsX482 and g.IVS19-2A>C in family 2. The c.1253delG mutation was associated with a c.1254C>A transversion. In vitro transcription analysis showed that exon 20 is skipped entirely when the g.IVS19-2A>C mutation is present. The wild-type glutamine residue at position 36 is strictly conserved.**

Conclusions: **Two previously unknown compound heterozygous mutations in the *DUOX2* gene, p.Q36H/p.S965fsX994 and p.G418fsX482/g.IVS19-2A>C, are responsible for iodide organification defects in 2 unrelated families. Identification of the molecular basis of this disorder might be helpful for understanding the pathophysiology of this congenital hypothyroidism.**

© 2006 American Association for Clinical Chemistry

Congenital hypothyroidism occurs with a prevalence of ~1 in 4000 newborns *(1, 2)*. Patients with this syndrome can be divided into 2 groups: those with nongoitrous (dysembryogenesis) and those with goitrous (dyshormonogenesis) congenital hypothyroidism. Dysembryogenesis, or dysgenesis, congenital hypothyroidism, which accounts for 85% of cases, results from ectopic thyroid tissue at the base of the tongue or in any position along the thyroglossal tract, agenesis, and hypoplasia. In a minority of these patients, the congenital hypothyroidism is associated with mutations in genes responsible for the development or growth of thyroid follicular cells: thyroid transcription factor 1 (*TTF-1*; also known as *TITF1*, *NKX2–1*, or *T/EBP*) *(3, 4)*, thyroid transcription factor 2 (*TTF-2*; also known as *TITF2*, *FOXE1*, or *FKHL15*) *(5)*, paired box transcription factor 8 (*PAX-8*) *(6–9)*, thyrotropin (*TSH*)[3] *(10, 11)*,

[1] Laboratorio de Biología Molecular, Cátedra de Genética y Biología Molecular, Facultad de Farmacia y Bioquímica, Universidad de Buenos Aires, Buenos Aires, Argentina.

[2] Centro de Investigaciones Endocrinológicas, CEDIE-CONICET, División Endocrinología, Hospital de Niños "Ricardo Gutiérrez", Buenos Aires, Argentina.

* Address correspondence to this author at: Laboratorio de Biología Molecular, Cátedra de Genética y Biología Molecular, Facultad de Farmacia y Bioquímica, Universidad de Buenos Aires, Av. Córdoba 2351, 4to piso-sala 5, 1120 Buenos Aires, Argentina. Fax 54-11-4508-3645; e-mail htargovn@huemul.ffyb.uba.ar.

Received July 26, 2005; accepted November 7, 2005.
Previously published online at DOI: 10.1373/clinchem.2005.058321

[3] Nonstandard abbreviations: TSH, thyrotropin; NIS, Na^+/I^- symporter; TG, thyroglobulin; TPO, thyroperoxidase; *DUOX* and Doux, dual oxidase gene (according to the recommendations of the Human Gene Nomenclature Committee) and protein; PDS, Pendrine; SSCP, single-strand conformational polymorphism; TT_4, total thyroxine; RT-PCR, reverse transcription-PCR; and TMD, transmembrane domain.

and TSH receptor *(12–14)*. The presence of congenital goiter (which accounts for the remaining 15% of cases) has been linked to mutations in the Na^+/I^- symporter (*NIS*) *(15–17)*, thyroglobulin (*TG*) *(18–21)*, thyroperoxidase (*TPO*) *(22–24)*, dual oxidase 2 (*DUOX2*; also known as *ThOX2* and *LNOX2*) *(25)*, and Pendrine (*PDS*; also known as *SLC26A4*) *(26, 27)* genes. These mutations produce a heterogeneous spectrum of congenital goitrous hypothyroidism, usually transmitted in an autosomal recessive mode.

Iodide organification defects are associated with mutations in the *TPO* or *DUOX2* genes *(22–25)* and are characterized by a positive perchlorate discharge test. TPO is the key enzyme in the formation of thyroid hormones; it catalyzes both the iodination and coupling of hormonogenic tyrosyl residues of TG with an absolute requirement of H_2O_2, which acts as an electron acceptor *(28)*. H_2O_2 is generated on the apical plasma membrane of the thyroid follicular cell by a metabolic pathway involving 2 members of the NADPH oxidase family: Duox1 and -2 *(29–34)*. The *DUOX2* gene (GenBank accession no. NT_010194) is located on chromosome 15q15.3 spanning 21.5 Kb of genomic DNA *(31)*, which includes 33 coding exons. The mRNA (GenBank accession no. NM_014080) is 6376 nucleotides long, and the preprotein is composed of a putative 26-amino acid signal peptide followed by a 1522-amino acid polypeptide *(31)*. The *DUOX1* gene encodes a homologous 1551-amino acid protein displaying 83% sequence similarity. To date, only 4 inactivating mutations in the *DUOX2* gene (p.R434X, p.Q686X, p.R701X, and p.S965fsX994) have been identified in patients with iodide organification defect *(25)*.

In the present study, screening by single-strand conformational polymorphism (SSCP) and direct sequencing analysis of the *DUOX2* gene revealed 3 previously unreported mutations and 1 previously reported mutation in 2 unrelated families with congenital goiter and iodide organification defect, constituting 2 compound heterozygous mutations (p.Q36H/p.S965fsX994 and p.G418fsX482/g.IVS19-2A>C).

Materials and Methods

PATIENT SELECTION

We studied 17 selected unrelated patients with iodide organification defect (perchlorate discharge test ≥30%) from an original cohort of 40 patients with congenital goitrous hypothyroidism at screening. We previously reported that 7 of these patients harbored mutations in the *TPO* gene: 1 was compound heterozygous, and the other 6 were simply heterozygous for the mutations *(24)*.

The project was approved by the Institutional Review Board, and written informed consent was obtained from all individuals involved in this study.

CLINICAL REPORT

Family 1: Index patient II-2. The patient is the second child of a nonconsanguineous couple and was referred because a high serum TSH value on neonatal screening at day 3 of life. He was born at term after an uncomplicated pregnancy and delivery with a birth weight of 3.1 kg. At day 27 of life, he had persistent jaundice, large posterior fontanel, and umbilical hernia. Thyroid tissue was palpable. After confirmation of hypothyroidism, he was started with L-thyroxine supplementation. At age 5 years, his thyroid hormone supplementation was interrupted for 4 weeks to investigate the etiology. A technetium-99 scan showed a goiter, and hypothyroidism was confirmed. His perchlorate discharge test result (46%) indicated a iodide organification defect. Treatment was reinitiated. He had a very good compliance, and his growth and development are normal. His parents and sister have normal thyroid function. The results of thyroid function tests of the members of family 1 who were studied are shown in Table 1.

Family 2: Patient II-2. The patient is the second child of a nonconsanguineous couple referred at the age of 8 months with hypothyroidism. She had all of the signs of thyroid hormone deficiency with goiter, and after confirmation, treatment with L-thyroxine was started.

At the age of 4.5 years, the etiology of her condition was assessed after withdrawal of the thyroxine supplementation, and hypothyroidism attributable to iodide organification defect was suspected (perchlorate discharge test result, 68%). She grew up normally but is mildly mentally retarded.

At age 15 years, after a noncomplicated pregnancy and delivery, she gave birth to a 3.0-kg male infant (III-1) who had a normal serum TSH concentration at neonatal screening for congenital hypothyroidism. The boy grew and developed normally up to 3 years of age when,

Table 1. Thyroid function test results for relatives and patients with congenital goitrous hypothyroidism and organification defect.[a]

Individuals	Serum TSH, mIU/L	Serum TT_4,[b] nmol/L	Serum TG, μg/L	Perchlorate discharge test, %
Family 1				
I-1	1.8	79.8	ND[c]	ND
I-2	2.7	109.4	ND	ND
II-1	2.5	105.5	14	5
II-2[d]	156	37.3	431	46
Family 2				
I-1	2.4	90.1	12	0
I-2	8.4	73.4	1.1	42
II-1	5.0	133.8	9.5	ND
II-2[d]	>100	10.3	479	68
II-3	6.2	109.4	1.5	ND
II-4[d]	>100	<12.87	1314	60
III-1	5.3/80[e]	119.7	84.2	31
Reference values	<5	77–180	2–30	<10

[a] See pedigrees in Fig. 1 for details.
[b] To convert nmol/L to μg/dL, divide by 12.87.
[c] ND, not determined.
[d] Affected individuals with organification defect.
[e] Basal value/value after treatment with thyrotropin-releasing hormone.

during a routine pediatric examination, a 30-g goiter was detected. Thyroid evaluation showed high serum TSH concentrations, a perchlorate discharge test result of 31%, and positive anti-thyroid antibodies [anti-TPO antibodies, 70 kIU/L (reference values <20 kIU/L]); anti-TG antibodies, 20 kIU/L (reference values <20 kIU/L)], indicating autoimmune thyroid disease.

Family 2: Index patient II-4. The patient was the fourth child of this family. He was referred at 1 month of age with severe hypothyroidism (persistent jaundice, myxedematous face, large posterior fontanel, and umbilical hernia) and goiter. Hypothyroidism was confirmed, and treatment with L-thyroxine was started. At age 4 years, the etiology of his condition was evaluated after withdrawal of thyroxine treatment. His findings resembled those of his sister.

The parents and the 2 healthy siblings of this family were evaluated. Thyroid function was normal in patient II-1, whereas the mother (I-2) and a sister (II-3) showed high serum TSH concentrations and positive anti-thyroid antibodies: for the mother (I-2), anti-TPO antibodies were 279 kIU/L and the anti-TG antibodies were <20 kIU/L; for the sister (II-3), the anti-TPO antibodies were 70 kIU/L and the anti-TG antibodies were 40 kIU/L. The perchlorate discharge test in I-2 was 42%. The father (I-1) had TSH concentrations within reference values and also positive anti-thyroid antibodies (anti-TPO antibodies, 64 kIU/L; anti-TG antibodies, 33 kIU/L. These findings indicate an autoimmune thyroid disease in I-1, I-2, and II-3.

The results of thyroid function tests of the family 2 members studied are shown in Table 1.

thyroid function tests

The perchlorate discharge test was performed according to standard procedures. Briefly, 25 μCi of radioiodine (I-131) was administered orally, and thyroid uptake was measured at 15-min intervals for 1 h. At this point, 500 mg of potassium perchlorate was given orally, and sequential uptakes were measured at 15-min intervals for an additional period of 2 h. Discharge was calculated as the difference between the uptake at the time of perchlorate administration and the uptake 120 min after perchlorate administration, expressed as a percentage. Values >10% were considered as a failure to retain the administered radioiodine, probably because of a congenital organification defect or an autoimmune thyroid disease.

Serum total thyroxine (TT_4) and serum TSH were determined by electrochemiluminescence immunoassay (ELECSYS™ system; Roche). Serum TG was measured by immunofluorometric assay (Delfia; Perkin-Elmer). Anti-TPO and anti-TG antibodies were measured by immunochemiluminometric assay (Immulite; Diagnostic Products Corporation).

SSCP analysis

SSCP analysis was used to screen for the presence of mutations in each exon of the *DUOX2* gene. Genomic DNA was isolated from leukocytes by the sodium dodecyl sulfate–proteinase K method. The complete coding sequence of the human *DUOX2* gene, along with the flanking intronic regions of each intron, were amplified from the affected patients. PCR was performed in 50-μL reactions containing a standard PCR buffer (Invitrogen, Life Technologies), 250 ng of genomic DNA, 1.5 or 2.5 mM $MgCl_2$, 200 μM each of dATP, dCTP, dTTP, and dGTP; with or without 80 nL/μL dimethyl sulfoxide; 1 U of Taq polymerase (Invitrogen, Life Technologies); and 40 pmol each of the forward and reverse primers. Intronic primers were specially designed or were as reported previously *(25)* for each of the 33 *DUOX2* coding exons. Their oligonucleotide sequences and the positions of their 5′ coding sequence ends are shown in Table 2. Samples were denatured at 95 °C for 3 min followed by 35 cycles of amplification, each consisting of denaturation at 95 °C for 30 s, primer annealing at 55–66 °C for 30 s, and primer extension at 72 °C for 1 min. After the last cycle, the samples were incubated for an additional 10 min at 72 °C to ensure that the final extension step was complete. The amplified products were analyzed in 2% agarose gels. The gel matrix for SSCP analysis contained 8% or 10% polyacrylamide (29:1; Invitrogen, Life Technologies), with or without 100 mL/L glycerol. Samples were electrophoresed for 18 h at a constant temperature (4 °C). DNA was visualized by silver staining.

DNA sequencing

Samples showing an aberrant pattern in SSCP analysis were directly sequenced with the Taq polymerase-based chain terminator method (*f*mol; Promega); the *DUOX2* forward and reverse primers were the same as those used in the SSCP screening (Table 2). The results were analyzed by use of the PC gene (Intelligenetics), DNASTAR (DNASTAR Inc.), and Nucleotide BLAST (http://www.ncbi.nlm.nih.gov/BLAST) software programs.

cloning of wild-type and mutated exon 11 PCR fragments

The amplified fragment corresponding to exon 11 from index patient II-4 (family 2) was T-A cloned into pGEM-T Easy vector (Promega). DH5α-competent cells were used for transformations. After transformation, the recombinant clones were identified by color screening on indicator plates containing isopropyl-thio-β-galactoside and 5-bromo-4-chloro-3-indolyl-β-D-galactoside (X-Gal), and plasmid DNA was isolated by standard procedures. DNA sequencing was performed as described above from wild-type and mutant allele clones.

validation of *DUOX2* mutations by SSCP analysis

We validated all mutations by studying healthy unrelated individuals by SSCP analysis under conditions identical to those described above, using the same intronic primers to amplify exons 2, 11, 20, and 21 (Table 2).

Table 2. *DUOX2* oligonucleotides used as primers in PCR amplification and sequence reactions.[a]

	Forward primers			Reverse primers	
Exon	Position of 5′ end	Nucleotide sequence, 5′→3′	Fragment size, bp	Position of 5′ end	Nucleotide sequence, 5′→3′
1	−170	tggcgtttggatgaaggt	300	+46	agggatcctggggaacac
2	−36	gtagctgggagcgtagtgct	226	+90	gtgttccccgcagattcc
3	−73	aggcttagggagaggtttgg	275	+36	cagatcaaccccactggtct
4	−23	tacggacggtttgtcacg	307	+89	cgcctctcccctccag
5	−34	ctcgacccgggctcac	246	+10	gtggcctcacCGTACAGC
6	−48	atcacgctaccgctcgtct	312	+97	tggcggttgtccacagat
7	−48	cccacaccatccaacttgtg	228	+119	gaaggagacggtgatgatgg
8	−54	aggatgtggaggcaagaa	250	+99	agtgaaactgcgaaggagtg
9	−104	aaggctcaatcctagtgaaccc	260	+65	tttcccagcctgtgtgaagaga
10	−39	tgggtagaggcctatcttga	218	+76	ctgctattgatgaacccagaggga
11	−44	atggagaggacaaagcccat	255	+47	gccataggaaagctttagctgc
12	−72	gagggatggggcaacagt	291	+43	aggctgaggagcagtctgag
13	−37	cttcccatcccagtgacttc	220	+65	gcaccctcaatcttgatcct
14	−66	gggaaagaggtctggccacata	301	+97	tgagcctggtctcaaacggt
15	−69	atagcctaagccacagtggagc	288	+105	aggtgccttggctttcctct
16	−46	ctggggacatctgctgaact	317	+68	gtggcctcgcttgtgataat
17	−126	caacccaagatccattgagg	326	+69	ttctatgcagcccaggtttc
18	−58	ttccagcataggcttcacct	319	+35	attcttggatagcctgccacct
19	−37	gcaaggagatgacctgcatt	204	+73	tcctctgactggacctgttt
20	−59	acctacccaagcctgaccttt	325	+69	cccaccaggaactctcattt
21	−34	ggaagccagtcctgcctctt	178	+74	gccagtcctactcccttcatt
22	−52	gttctcctggctgcaaagac	213	+77	gatatgtgggtggggccta
23	−59	cattaagggaaggccagagg	305	+67	gctttccactcctctccaag
24	−37	cctgtgccaagctgatgtaa	305	+37	gctgcagcaaagaggaagaa
25	−44	agtctgtcctggttggcatc	184	+40	caccctatgagtcccaggag
26	−65	gtgttgtgacagtgctggag	208	+93	cccatggccagtatagacaag
27	−57	tttcagcccaagctgaagtc	254	+69	tccctctttcaccttcctgt
28	−26	gttgtactaactggccgtgt	287	+107	acagagtcagaggcagtgat
29	−45	gagcaggccttctcatctgt	345	+67	atagggaagggcagagatcc
30	−39	cagggtcaggctcatttcat	251	+53	gtcacaattcggccacctat
31	−53	atctagggaggctgaactga	266	+57	ttacgctgccaatccatctg
32	−82	ctgtctcttgggctatgtgg	319	+108	caatcgggtggagttctctg
33	−58	caaggagagtgagcaccttt	286	4955	AGGCCTAAGGTGGATTCTGA

[a] Exons sequences are in uppercase, introns sequences are in lowercase. The intronic nucleotide position is numbered from the exon end: negative numbers start from the g of the ag splice acceptor site; positive numbers start from the g of the gt splice donor site.

*Aci*I restriction analysis

The mutant cytosine, detected by nucleotide sequencing in position 108 (p.Q36H), creates a new *Aci*I restriction site that is absent in the wild-type allele, which has guanine at position 108. The presence of the mutation was therefore independently confirmed by restriction analysis with *Aci*I (New England BioLabs Inc.) in index patient II-2 (family 1) and his sister and parents. A 226-bp fragment containing exon 2 was generated by PCR under conditions identical to those described above with the same exon 2 intronic primers (Table 2). The PCR product (1 μg) was digested overnight at 37 °C with 10 U of *Aci*I. After digestion, the DNA fragments were separated on a 2% agarose gel and visualized with ethidium bromide. Digestion of the mutant allele produced 2 fragments of 142 and 84 bp.

construction and expression of the minigenes

To study the effect of the g.IVS19-2A>C mutation, we constructed wild-type and mutated minigenes, using the exon trapping vector pSPL3 (Life Technologies). The genomic DNA region from index patient II-4 (family 2) between exons 18 and 22 and the intronic flanking sequences (158 bp upstream from the 5′ exon 18 end and 156 bp downstream from the 3′ exon 22 end) were amplified by long PCR, as described previously *(35)*. The forward primer (pSPL3-In17F; 5′-CACCGAATGCGGCCGCAACAGAGGCCCCAGTCAGTA-3′) contained the *Not*I site, and the reverse primer (pSPL3-In22R; 5′-GCGGATCCGAGACTCAGGATGGTCGCTT-3′) contained the *Bam*HI site. The 3900-bp (3876 of which were *DUOX2* sequences) PCR products were purified from the agarose gel by use if the GFX PCR DNA and Gel Band Purification Kit

(Amersham Biosciences) and were sequentially digested with *Not*I and *Bam*HI. The insert was directionally cloned into the *Not*I and *Bam*HI sites of the pSPL3 vector. Because index patient II-4 (family 2) is heterozygous for the IVS19-2A>C mutation, the wild-type and mutated alleles were thus cloned. The recombinant plasmids were amplified in DH5α-competent cells and purified by use of the Concert High Purity Plasmid Miniprep System (Life Technologies). The correct sequence was confirmed by sequencing with the intronic forward primer used for PCR amplification of exon 20 (Table 2).

CV-1 cells were grown in 3.8-cm dishes in DMEM supplemented with 50 mL/L bovine calf serum and 100 kIU/L penicillin–streptomycin in a 5% CO_2 atmosphere at 37 °C. When the cells reached ~90% confluence, they were transfected with 1 μg of plasmid DNA (wild-type, mutant, and control pSPL3) per 3.8-cm dish with Lipofectamine 2000 (Invitrogen, Life Technologies). After incubation for 48 h, the cells were harvested and total RNA was extracted with Trizol (Invitrogen, Life Technologies). Reverse transcription-PCR (RT-PCR) was performed in the SuperScript One-Step RT-PCR System (Invitrogen, Life Technologies) with the exon 18 forward primer (e18F; 5′-TGACAAGGATGGCAATGGCT-3′) and the exon 22 reverse primer (e22R; 5′-GCCAAACCTCTTCTTCAGTCCA-3′). Samples were incubated at 45 °C for 50 min, then at 94 °C for 10 min, followed by 40 cycles of DNA denaturation (94 °C for 45 s), annealing (55 °C for 1 min), and polymerization (72 °C for 1 min). After the last cycle, the samples were incubated for an additional 10 min at 72 °C. The RT-PCR products were purified from the agarose gel by use of the GFX PCR DNA and Gel Band Purification Kit (Amersham Biosciences) and then direct sequenced with the e18F and e22R primers.

PROTEIN ANALYSIS

We compared amino acid sequence homologies between several species of Duox2 and Duox1 families, using the Protein Blast and Search for Conserved Domains (http://www.ncbi.nlm.nih.gov/BLAST) software programs.

Results

SCREENING OF MUTATIONS IN THE *DUOX2* GENE BY SSCP AND SEQUENCE ANALYSIS

All 33 coding exons of the *DUOX2* gene, along with the flanking intronic sequences, from 17 unrelated patients with iodide organification defect and healthy controls were screened by SSCP analysis. Analysis of PCR products showed 4 different patterns of migration in 2 patients (II-2 in family 1 and II-4 in family 2) that were not detected in the healthy controls. The remaining 15 unrelated patients did not show aberrant bands, suggesting the absence of *DUOX2* gene mutations. Sequence analysis of the samples showing the abnormal SSCP patterns revealed 3 previously unreported mutations and 1 previously identified mutation (c.2895-2898delGTTC) *(25)*. One was a missense mutation involving a guanine-to-cytosine transition at nucleotide 108 in exon 2 (c.108G>C), which replaces the wild-type glutamine at codon 36 with a histidine (p.Q36H; see Fig. 1 in the Data Supplement that accompanies the online version of this article at http://www.clinchem.org/content/vol52/issue2/). The second was a guanine deletion at nucleotide 1253 in exon 11 (c.1253delG), which produced a frameshift at amino acid 418 in exon 11 with a putative premature stop codon at amino acid position 482 in exon 12 (p.G418fsX482; see Fig. 2 in the online Data Supplement). The third was a adenine-to-cytosine transversion at position −2 of the splice acceptor site in intron 19 (g.IVS19-2A>C; see Fig. 3 in the online Data Supplement). This infers the possibility that the splice-site mutation might lead to total elimination of exon 20 of the *DUOX2* gene. Translation of the resulting mutated transcript showed that the reading frame was not maintained by the junction of exons 19 and 21 and that, consequently, a frameshift was generated with a putative premature stop codon at amino acid position 886 in exon 21.

The last mutation detected by SSCP analysis was a previously reported GTTC deletion in exon 21 (c.2895-2898delGTTC) *(25)*, which causes a frameshift at amino acid 965 in exon 21 with a putative premature stop codon at amino acid position 994 in exon 22 (p.S965fsX994; see Fig. 4 in the online Data Supplement).

These findings indicate that index patient II-2 (family 1) is compound heterozygous for p.Q36H/p.S965fsX994, whereas index patient II-4 (family 2) is compound heterozygous for p.G418fsX482/g.IVS19-2A>C.

The c.1253delG heterozygous state of index patient II-4 was confirmed by cloning and sequencing of both wild-type and mutant alleles. Another difference identified in the mutant allele was a cytosine-to-adenine transversion in position 1254 (c.1254C>A; see Fig. 2 in the online Data Supplement).

Previous SSCP analysis did not show evidence of *TPO* gene mutations in either index patient (II-2 in family 1 and II-4 in family 2) *(24)*.

VALIDATION OF *DUOX2* MUTATIONS BY SSCP ANALYSIS

We ruled out the possibility that the p.Q36H mutation could be a polymorphism because it was not detected in 134 chromosomes from the general population by SSCP analysis (data not shown). The p.G418fsX482 and g.IVS19-2A>C mutations were not detected in 100 alleles from healthy individuals screened by SSCP analysis. In contrast, 1 of the 200 chromosomes also analyzed by SSCP had the p.S965fsX994 mutation (data not shown).

SEGREGATION ANALYSIS OF *DUOX2* MUTATIONS IN FAMILY 1

SSCP analysis of PCR products of exons 2 and 21 from index patient II-2, his father (I-1), his mother (I-2), and his unaffected sister (II-1; Fig. 1) showed that II-2 inherited 1 copy of the p.Q36H mutation from his mother and 1 copy

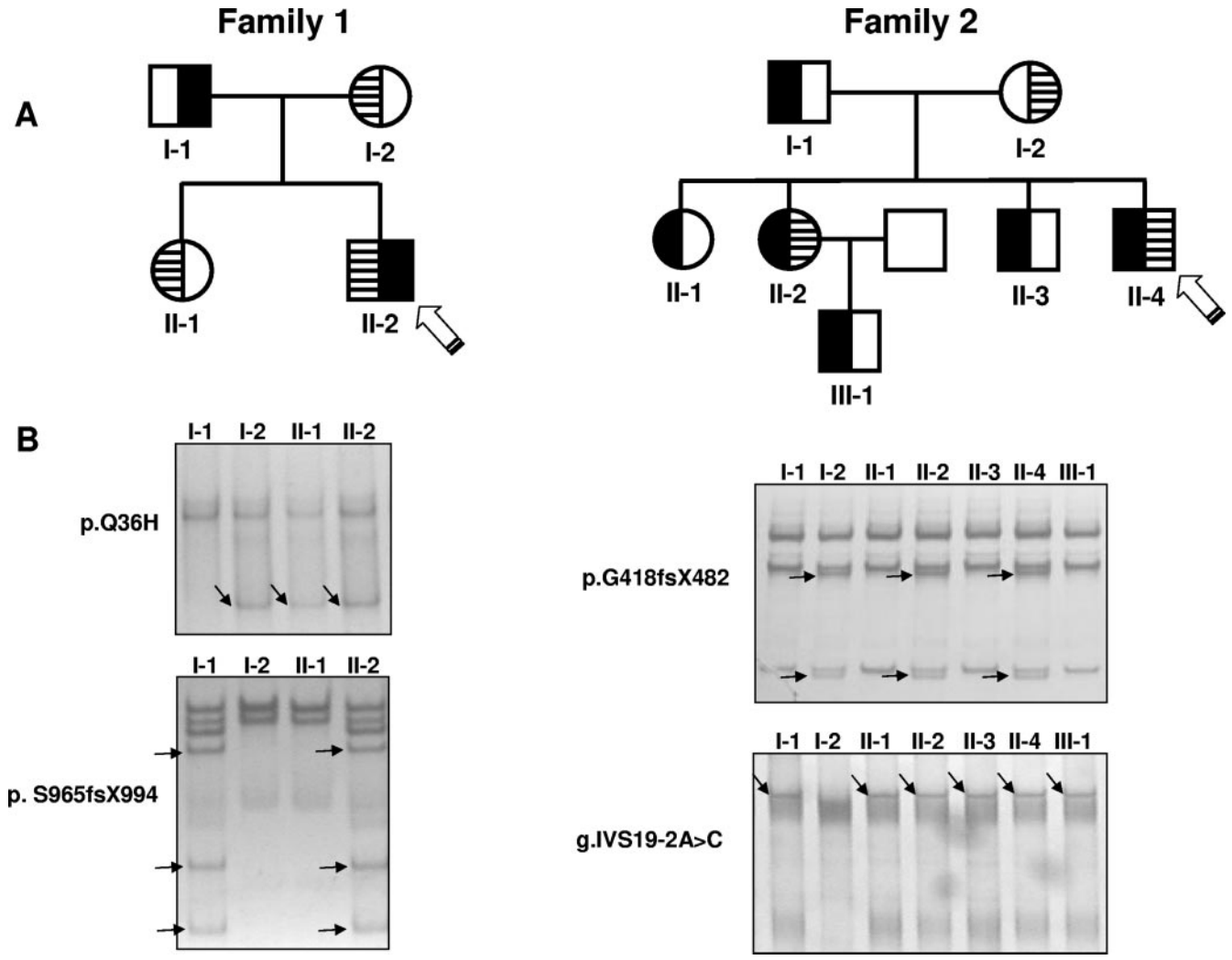

Fig. 1. Segregation analysis of the *DUOX2* mutated alleles in members of families 1 and 2.

(*A*), pedigrees showing the pattern of inheritance of the *DUOX2* mutated alleles. *Squares* and *circles* indicate male and female members, respectively. *Filled symbols* denote affected patients; *half-filled symbols*, unaffected heterozygote individuals. The *open arrows* indicate the index patients (II-2 in family 1 and II-4 in family 2). In family 1, the *striped symbols* indicate the p.Q36H allele, and the *filled symbols* the p.S965fsX994 allele. In family 2, the *striped symbols* indicate the p.G418fsX482 allele, and the *filled symbols* the g.IVS19-2A>C allele. (*B*), SSCP analysis of exons 2, 11, 20, and 21. The PCR products were subjected to electrophoresis in 8%–10% nondenaturing acrylamide gels without glycerol. The *filled arrows* indicate the aberrant migration bands.

of the p.S965fsX994 mutation from his father. The healthy sister (II-1) was heterozygous for the p.Q36H mutation and did not carry the p.S965fsX994 mutation (Fig. 1).

The guanine-to-cytosine transversion at position 108 creates a restriction site for *Aci*I. The index patient II-2, his mother, and his unaffected sister (II-1) have a wild-type allele (226 bp) containing guanine at position 108, which is resistant to digestion with *Aci*I, and a mutant allele containing cytosine at position 108, which is digested with *Aci*I, producing 2 fragments of 142 and 84 bp. In contrast, the father has only the wild-type sequence at this position (data not shown).

segregation analysis of *DUOX2* mutations in family 2

SSCP analysis of PCR products of exons 11 and 20 from index patient II-4, his father (I-1), his mother (I-2), his unaffected sister (II-1), his unaffected brother (II-3), his affected sister (II-2), and the unaffected nephew (III-1; Fig. 1) showed that both affected siblings II-2 and II-4 inherited 1 copy of the p.G418fsX482 mutation from their mother and 1 copy of the g.IVS19-2A>C mutation from their father. The healthy sister and brother (II-1 and II-3) and the unaffected nephew (III-1) were heterozygous for the g.IVS19-2A>C mutation and did not carry the p.G418fsX482 mutation (Fig. 1).

minigene analysis

Using the exon trapping system, we tested a minigene containing the g.IVS19-2A>C mutation for abnormal splicing. In vitro transcription showed that exon 20, which consists of 197 bp, is skipped entirely when the g.IVS19-2A>C mutation is present, whereas the minigene that contains the wild-type allele is correctly spliced (Fig. 2).

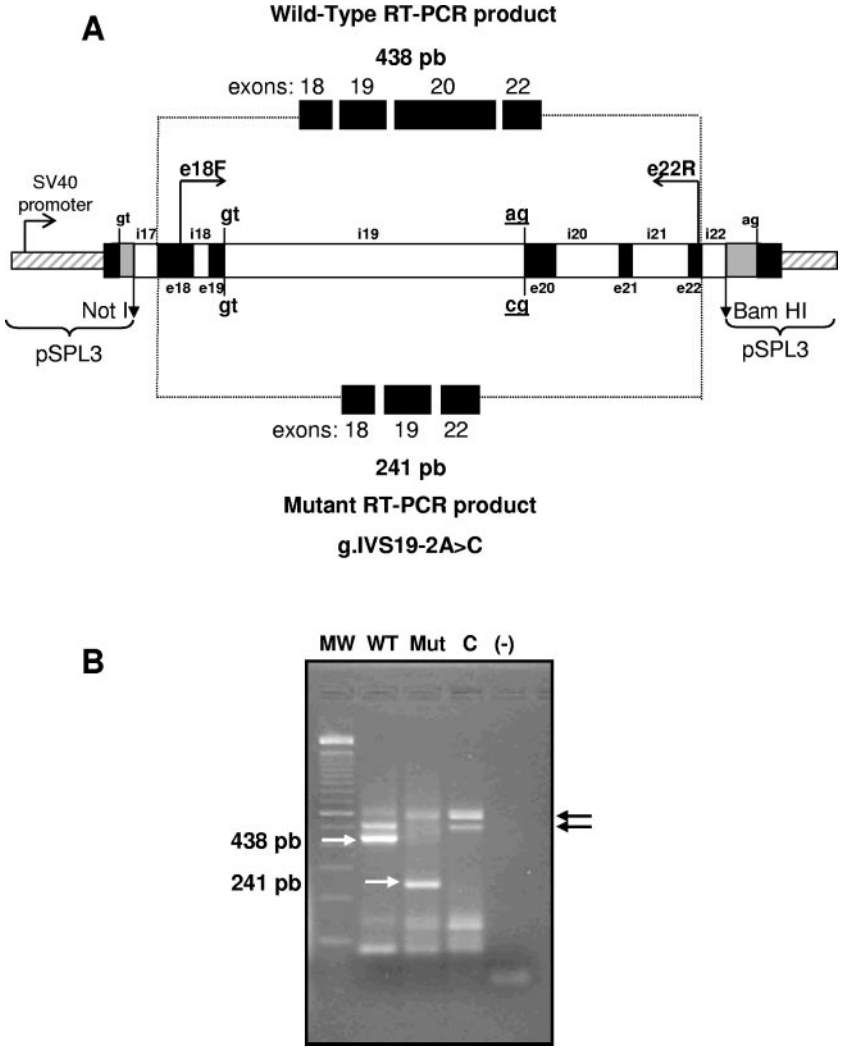

Fig. 2. In vitro expression of the wild-type and mutant g.IVS19-2A>C minigenes.

(*A*), schematic representation of the genomic organization of the wild-type and mutant minigenes and their RT-PCR products. The 3876-bp PCR amplified fragments from index patient II-4 (family 2) were directionally cloned into the *Not*I and *Bam*HI sites of the exon-trapping pSPL3 vector, which was produced in CV-1 cells. Vector and genomic DNA splice donor (*gt*) and acceptor (*ag*) sites are shown. cDNA was synthesized from transcribed mRNA and amplified with primers e18F and e22R, located in exons 18 and 22 of the *DUOX2* gene, respectively. Processing of the wild-type transfected sequences produced a majority PCR product of 438 bp. In contrast, the IVS19-2A>C mutation leads to the skipping of exon 20, producing a 241-bp fragment. (*B*), agarose electrophoresis of the RT-PCR products. The RT-PCR fragments from wild-type (*WT*) and mutant (*Mut*) minigenes, pSPL3 vector control (*C*) and the negative PCR control (−) were electrophoresed on a 2% agarose gel, stained with ethidium bromide, and visualized under ultraviolet light. The nonspecific PCR bands are indicated by *filled arrows*. The DNA size marker (*MW*) was a 100-bp DNA ladder (Invitrogen, Life Technologies).

Interestingly, RT-PCR amplification products of both minigenes lacked exon 21. Two nonspecific PCR bands were detected in the pSPL3 vector control and in both wild-type and mutant minigenes (Fig. 2B).

PROTEIN ANALYSIS

Comparison of the human Duox2 with sequences found in the GenBank database, using the Blast network service, revealed that the wild-type glutamine residue at position 36 was strictly conserved in all Duox1 and Duox2 species analyzed (Fig. 3).

Discussion

An organification defect attributable to *DUOX2* gene mutations is one of the causes for thyroid dyshormonogenesis *(25)*. This type of primary congenital hypothyroidism is characterized by intact iodide trapping, normal TG protein, and aberrant organification of iodide *(1, 2)*. In

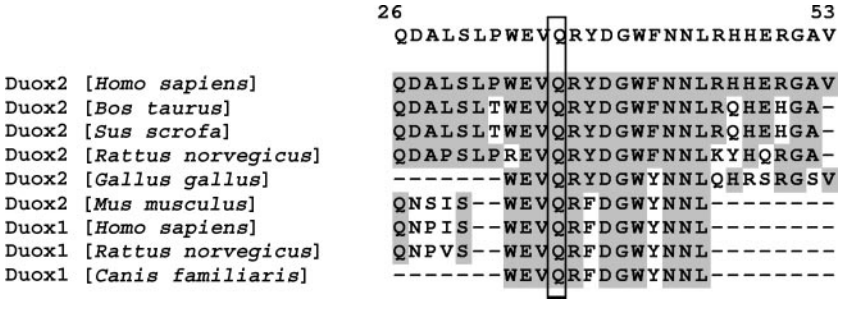

Fig. 3. Protein homology analysis.

Shown is the partial protein alignment of the different species of the Duox2 and Duox1 families. Conserved residues are indicated by *gray shading*, and the glutamine residue at position 36, involved in the missense mutation (p.Q36H), is *boxed*.

this study, all 3 affected individuals had clinical and biochemical criteria suggestive of congenital goiter associated with deficiency in the organification of iodide: presence of goiter, hypothyroidism, positive perchlorate discharge test, and high serum TG and TSH concentrations with simultaneous low serum TT_4 concentrations *(1, 2)*. Molecular analyses indicated that the affected individuals carry either compound heterozygous mutations for p.Q36H/p.S965fsX994 or p.G418fsX482/g.IVS19-2A>C.

Duox2 contains 7 transmembrane domains (TMDs), a domain of homology with peroxidase (TPO-like), 5 potential sites for N-glycosylation, 1 conserved arginine and 4 specific histidines involved in the heme prosthetic group binding, 1 FAD- and 4 NADPH-binding sites, and 2 EF-hand domains *(31–34)* (see Fig. 5A in the online Data Supplement). The p.Q36H missense mutation is located in the TPO-like domain of Duox2 (see Fig. 5B in the online Data Supplement). The putative function of the peroxidase homology domain is not yet clear. Edens et al. *(36)* reported that the TPO-like domain of Duox1 catalyzes protein cross-linking by forming dityrosine bonds. The p.Q36H mutation was not detected in the general population, suggesting that this change is not a polymorphism. More importantly, the wild-type glutamine residue at position 36 is strictly conserved in all species for which suitable Duox1 and Duox2 sequences have been reported. On the basis of such observations, we hypothesize that the glutamine residue in this position plays a critical structural role in the Duox2 protein. Consequently, the p.Q36H mutation may cause structural instability leading to deficient Duox2 function.

The putative truncated protein of 481 amino acids generated by the c.1253delG mutation (p.G418fsX482) eliminates the last 2 potential sites for N-glycosylation, both EF-hand domains, all histidine and arginine sites, all TMDs, and the FAD- and NADPH-binding sites (see Fig. 5C in the online Data Supplement), whereas the putative truncated protein of 993 amino acids generated by the c.2895–2898delGTTC mutation (p.S965fsX994) eliminates all histidine and arginine sites, the last 6 TMDs, and the FAD- and NADPH-binding sites (see Fig. 5E in the online Data Supplement). We found the c.1253delG mutation associated with the c.1254C>A transversion in the same allele. This substitution was not detected in any of the 100 alleles from healthy individuals screened by SSCP analysis, suggesting that it is not a polymorphic nucleotide position. However, a hypothetical allele with the c.1254C>A transversion and without the c.1253delG mutation would conserve glycine-418 (GGC>GGA). The functional consequences of both truncated proteins, on the one hand, is insufficient thyroidal production of H_2O_2, which prevents the synthesis of sufficient quantities of thyroid hormones. On the other hand, deletion of the middle region and/or C-terminal of Duox2 could alter the protein folding and assembly, leading to a marked reduction in the ability to export the protein from the endoplasmic reticulum *(37, 38)*. An interesting but unsolved question, which could not be investigated because the thyroid tissue from patients was unavailable and we thus could not perform mRNA analysis, would have been to estimate the *DUOX2* transcript concentration in goiters. In general, mRNA containing nonsense mutations is found in low concentrations. This decrease is attributable to an accelerated degradation rate of the mutated mRNA because the untranslated part of the messenger is not protected by ribosomes. To complement this scenario, it is not possible to exclude that an alternative splicing mechanism, by activation of cryptic splice sites, might restore the normal reading frame disrupted by the mutation and eliminate the stop codon that would truncate the protein. As is reported for the human *TPO* gene, a GGCC insertion-duplication at position 1186 in the eighth exon (p.R396fsX472) would lead to a frameshift at amino acid 396 with a premature stop at 472 in exon 9 *(22)*. Alternative splicing by a cryptic acceptor splice site in exon 9 restores the normal reading frame disrupted by the mutation and eliminates the stop codon.

Another mutation found in this study is a previously unreported A-to-C transversion at position −2 in the acceptor site of intron 19. This splice site mutation might lead to total elimination of exon 20 of the *DUOX2* gene. It is known from other genes that mutations in this site that alter the consensus acceptor site can lead to exon skipping *(18)*. Because of the thyroid tissue from II-4 is unavailable, we used an in vitro exon-trapping system to evaluate whether the g.IVS19-2A>C mutation produces an abnormal transcript by a defect in exon splicing. We found that during in vitro transcription, the mutation in the acceptor splice site causes skipping of exon 20. The excision of exon 20 in the *DUOX2* mRNA might generate a frameshift with a putative premature stop codon in exon 21, which encodes a grossly truncated protein of 885 amino acids. The premature stop eliminates all histidine and arginine sites, the last 6 TMDs, and the FAD- and NADPH-binding sites (see Fig. 5D in the online Data Supplement). Unexpectedly, the RT-PCR products of both wild-type and mutant minigenes lacked the sequence corresponding to exon 21. At present, there are no published reports referring to the existence of alternatively spliced mRNAs lacking exon 21 of the *DUOX2* gene. However, the excision of exons 20 and 21 would restore the normal reading frame in the mutated allele. Further experiments are required to confirm excision of exon 21 in the mRNA and to determine their functional consequences.

Finally, it is interesting to note that patient II-2 (family 1), who carries a missense mutation in one allele and a putative premature stop codon in the other allele (p.Q36H/p.S965fsX994), had a perchlorate discharge test result of 46%, whereas patients II-2 and II-4 (family 2), who carry 2 putative premature stop codons, one in each allele (p.G418fsX482/g.IVS19-2A>C), have major iodide discharges: 68% and 60%, respectively. Subsequently, we

could hypothesize that the p.Q36H mutation causes a slight reduction in Duox2 function. However, the positive perchlorate discharge test observed in members I-2 (42%) and III-1 (31%) of family 2, both heterozygous for the p.G418fsX482 and g.IVS19-2A>C mutations, respectively, could be caused for their autoimmune thyroid diseases.

From our study, we can draw 5 conclusions: (*a*) SSCP analysis of the entire coding sequence of the human *DUOX2* gene, including the flanking intronic regions, and sequencing of the fragments presenting aberrant migration patterns revealed 3 previously unreported mutations (p.Q36H, p.G418fsX482, and g.IVS19-2A>C) and 1 previously reported mutation (p.S965fsX994). (*b*) These finding established the inheritance in 2 unrelated family of 2 compound heterozygous mutations (p.Q36H/p.S965fsX994 and p.G418fsX482/g.IVS19-2A>C). (*c*) Analysis of the GenBank database revealed that the wild-type glutamine residue at position 36 is strictly conserved. (*d*) In vitro transcription analysis confirmed that exon 20 is skipped entirely when the g.IVS19-2A>C mutation is present. (*e*) The p.S965fsX994 mutation is the most frequent mutation in the *DUOX2* gene; consequently, it would be helpful to investigate further cases with congenital hypothyroidism regarding this mutation. The identification and characterization of an increasing number of natural mutations have provided important insights into the structure–function relationship of Duox2.

C.M. Rivolta and H.M. Targovnik are established investigators of the Consejo Nacional de Investigaciones Científicas y Técnicas (CONICET). S.A. Esperante is a research fellow of the Agencia Nacional de Promoción Científica y Tecnológica-Fondo para la Investigación Científica y Tecnológica (ANPCyT-FONCyT). This work was supported by grants from Universidad de Buenos Aires (B 087/2001 and B 057/2004) and ANPCyT-FONCyT (05-08838/PICT 2000/2001)

References

1. Medeiros-Neto G, Knobel M, DeGroot LJ. Genetic disorders of the thyroid hormone system. In: Baxter JD, ed. Genetics in endocrinology. Philadelphia: Lippincott Williams & Wilkins, 2002:375–402.
2. Knobel M, Medeiros-Neto G. An outline of inherited disorders of the thyroid hormone generating system [Review]. Thyroid 2003; 13:771–801.
3. Pohlenz J, Dumitrescu A, Zundel D, Martiné U, Schönberger W, Koo E, et al. Partial deficiency of thyroid transcription factor 1 produces predominantly neurological defects in humans and mice. J Clin Invest 2002;109:469–73.
4. Krude H, Schütz B, Biebermann H, von Moers A, Schnabel D, Neitzel H, et al. Choreoathetosis, hypothyroidism, and pulmonary alterations due to human NKX2–1 haploinsufficiency. J Clin Invest 2002;109:475–80.
5. Clifton-Bligh RJ, Wentworth JM, Heinz P, Crisp MS, John R, Lazarus JH, et al. Mutation of the gene encoding human TTF-2 associated with thyroid agenesis, cleft palate and choanal atresia. Nat Genet 1998;19:399–401.
6. Macchia PE, Lapi P, Krude H, Pirro MT, Missero C, Chiovato L, et al. PAX8 mutations associated with congenital hypothyroidism caused by thyroid dysgenesis. Nat Genet 1998;19:83–6.
7. Vilain C, Rydlewski C, Duprez L, Heinrichs C, Abramowicz M, Malvaux P, et al. Autosomal dominant trasmission of congenital thyroid hypoplasia due to loss-of-function mutation of PAX8. J Clin Endocrinol Metab 2001;86:234–8.
8. Congdon T, Nguyen LQ, Nogueira CR, Habiby RL, Medeiros-Neto G, Kopp P. A novel mutation (Q40P) in PAX8 associated with congenital hypothyroidism and thyroid hypoplasia: evidence for phenotypic variability in mother and child. J Clin Endocrinol Metab 2001;86:3962–7.
9. Meeus L, Gilbert B, Rydlewski C, Parma J, Roussie AL, Abramowicz M, et al. Characterization of a novel loss of function mutation of PAX8 in a familial case of congenital hypothyroidism with in-place, normal-sized thyroid. J Clin Endocrinol Metab 2004;89:4285–91.
10. Pohlenz J, Dumitrescu A, Aumann U, Koch G, Melchior R, Prawitt D, et al. Congenital secondary hypothiroidism caused by exon skipping due to a homozygous donor splice site mutation in the TSHβ-subunit gene. J Clin Endocrinol Metab 2002;87:336–9.
11. Borck G, Topaloglu AK, Korsch E, Martiné U, Wildhardt G, Onenli-Mungan N, et al. Four cases of congenital secondary hypothyroidism due to a splice site mutation in the thyrotropin-β gene: phenotypic variability and founder effect. J Clin Endocrinol Metab 2004;89:4136–41.
12. Sunthornthepvarakul T, Gottschalk ME, Hayashi Y, Refetoff S. Resistance to thyrotropin caused by mutations in the thyrotropin-receptor gene. N Engl J Med 1995;332:155–60.
13. Abramowicz MJ, Duprez L, Parma J, Vassart G, Heinrichs C. Familial congenital hypothyroidism due to inactivating mutation of the thyrotropin receptor causing profound hypoplasia of the thyroid gland. J Clin Invest 1997;99:3018–24.
14. Tonacchera M, Agretti P, Pinchera A, Rosellini V, Perri A, Collecchi P, et al. Congenital hypothyroidism with impaired thyroid response to thyrotropin (TSH) and absent circulating thyroglobulin: evidence for a new inactivating mutation of the TSH receptor gene. J Clin Endocrinol Metab 2000;85:1001–8.
15. Miki K, Harada T, Miyai K, Takai S-I, Amino N. Congenital hypothyroidism caused by a mutation in the Na^+/I^- symporter. Nat Genet 1997;16:124–5.
16. Pohlenz J, Medeiros-Neto G, Gross JL, Silveiro SP, Knobel M, Refetoff S. Hypothyroidism in a Brazilian kindred due to iodide trapping defect caused by homozygous mutation in the sodium/iodide symporter gene. Biochem Biophys Res Commun 1997; 240:488–91.
17. Pohlenz J, Rosenthal IM, Weiss RE, Jhiang SM, Burant C, Refetoff S. Congenital hypothyroidism due to mutations in the sodium/iodide symporter: identification of a nonsense mutation producing a downstream cryptic 3′ splice site. J Clin Invest 1998;101: 1028–35.
18. Ieiri T, Cochaux P, Targovnik HM, Suzuki M, Shimoda S-I, Perret J, et al. A 3′ splice site mutation in the thyroglobulin gene responsible for congenital goiter with hypothyroidism. J Clin Invest 1991;88:1901–5.
19. Caron P, Moya CM, Malet D, Gutnisky VJ, Chabardes B, Rivolta CM, et al. Compound heterozygous mutations in the thyroglobulin gene (1143delC and 6725G→A[R2223H]) resulting in fetal goitrous hypothyroidism. J Clin Endocrinol Metab 2003;88:3546–53.
20. Gutnisky VJ, Moya CM, Rivolta CM, Domené S, Varela V, Toniolo JV, et al. Two distinct compound heterozygous constellation (R277X/IVS34-1G>C and R277X/R1511X) in the thyroglobulin (TG) gene in affected individuals of a Brazilian kindred with congenital goiter and defective TG synthesis. J Clin Endocrinol Metab 2004;89:646–57.
21. Rivolta CM, Moya CM, Gutnisky VJ, Varela V, Miralles-García JM,

González-Sarmiento R, et al. A new case of congenital goiter with hypothyroidism due to a homozygous p.R277X mutation in the exon 7 of the thyroglobulin gene: a mutational hot spot could explain the recurrence of this mutation. J Clin Endocrinol Metab 2005;90:3766–70.

22. Abramowicz MJ, Targovnik HM, Varela V, Cochaux P, Krawiec L, Pisarev MA, et al. Identification of a mutation in the coding sequence of the human thyroid peroxidase gene causing congenital goiter. J Clin Invest 1992;90:1200–4.

23. Bakker B, Bikker H, Vulsma T, de Randamie JSE, Wiedijk BM, de Vijlder JJM. Two decades of screening for congenital hypothyroidism in the Netherlands: TPO gene mutations in total iodide organification defect (an update). J Clin Endocrinol Metab 2000; 85:3708–12.

24. Rivolta CM, Esperante SA, Gruñeiro-Papendieck L, Chiesa A, Moya CM, Domené S, et al. Five novel inactivating mutations in the human thyroid peroxidase gene responsible for congenital goiter and iodide organification defect. Hum Mutat 2003;22:259. Available from http://www.interscience.wiley.com/humanmutation/pdf/mutation/646.pdf.

25. Moreno JC, Bikker H, Kempers MJE, van Trotsenburg ASP, Baas F, de Vijlder JJM, et al. Inactivating mutations in the gene for thyroid oxidase 2 (THOX2) and congenital hypothyroidism. N Engl J Med 2002;347:95–102.

26. Kopp P. Pendred syndrome and genetic defects in thyroid hormone synthesis [Review]. Rev Endocr Metab Disord 2000;1:109–21.

27. Borck G, Roth C, Martiné U, Wildhardt G, Pohlenz J. Mutations in the PDS gene in German families with Pendred's syndrome: V138F is a founder mutation. J Clin Endocrinol Metab 2003;88: 2916–21.

28. Taurog A. Hormones synthesis. In: Braverman LE, Utiger RD, eds. Wernwe and Ingbar's the thyroid, 8th ed. Philadelphia: Lippincott Raven, 2000:61–85.

29. Dupuy C, Ohayon R, Valent A, Noel-Hudson MS, Deme D, Virion A. Purification of a novel flavoprotein involved in the thyroid NADPH oxidase. Cloning of the porcine and human cDNAs. J Biol Chem 1999;274:37265–9.

30. Leseney AM, Deme D, Legue O, Ohayon R, Chanson P, Sales JP, et al. Biochemical characterization of a Ca^{2+}/NAD(P)H-dependent H_2O_2 generator in human thyroid tissue. Biochimie 1999;81:373–80.

31. De Deken X, Wang D, Many MC, Costagliola S, Libert F, Vassart G, et al. Cloning of two human thyroid cDNAs encoding new members of the NADPH oxidase family. J Biol Chem 2000;275:23227–33.

32. De Deken X, Wang D, Dumont JE, Miot F. Characterization of ThOX proteins as components of the thyroid H_2O_2-generating system. Exp Cell Res 2002;273:187–96.

33. Lambeth JD, Cheng G, Arnold RS, Edens WA. Novel homologs of gp91phox. Trends Biochem Sci 2000;25:459–61.

34. Krause KH. Tissue distribution and putative physiological function of NOX family NADPH oxidases [Review]. Jpn J Infect Dis 2004; 57:S28–9.

35. Moya CM, Varela V, Rivolta CM, Mendive FM, Targovnik HM. Identification and characterization of a novel large insertion/deletion polymorphism of 1464 base pair in the human thyroglobulin gene. Thyroid 2003;13:319–23.

36. Edens WA, Sharling L, Cheng G, Shapira R, Kinkade JM, Lee T, et al. Tyrosine cross-linking of extracellular matrix is catalyzed by Duox, a multidomain oxidase/peroxidase with homology to the phagocyte oxidase subunit gp91phox. J Cell Biol 2001;154:879–92.

37. Morand S, Dos Santos OF, Ohayon R, Kaniewski J, Noel-Hudson MS, Virion A, et al. Identification of a truncated dual oxidase 2 (DUOX2) messenger ribonucleic acid (mRNA) in two rat thyroid cell lines: insulin and forskolin regulation of DUOX2 mRNA levels in FRTL-5 cells and porcine thyrocytes. Endocrinology 2003;144: 567–74.

38. Morand S, Agnandji D, Noel-Hudson MS, Nicolas V, Buisson S, Macon-Lemaitre L, et al. Targeting of the dual oxidase 2 N-terminal region to the plasma membrane. J Biol Chem 2004;279: 30244–51.